VTT Technical Research Centre of Finland

BEAVRS pin-by-pin calculations with Ants-SUBCHANFLOW-SuperFINIX code system

Tuominen, Riku; Valtavirta, Ville

Published in:
Annals of Nuclear Energy

DOI:
10.1016/j.anucene.2022.109447

Published: 01/01/2023

Document Version
Publisher's final version

Annals of Nuclear Energy 180 (2023) 109447

Contents lists available at ScienceDirect

Annals of Nuclear Energy

journal homepage: www.elsevier.com/locate/anucene

BEAVRS pin-by-pin calculations with Ants-SUBCHANFLOW-SuperFINIX code system

Riku Tuominen *, Ville Valtavirta

VTT Technical Research Centre of Finland Ltd., P.O. Box 1000, FI-02044 VTT, Finland

ARTICLE INFO

Keywords:
Ants
Multi-physics
Kraken
Depletion

ABSTRACT

In this work the nodal neutronics code Ants is coupled with the subchannel code SUBCHANFLOW and the fuel behavior code SuperFINIX within VTT's Kraken framework in order to evaluate thermal margins. The coupling is implemented using Cerberus which is the multi-physics driver of Kraken. The capabilities of the new coupled code system are demonstrated by modeling the first operating cycle of BEAVRS. Calculated and measured boron concentrations are compared and selected pin-by-pin results are presented at 3 points during the operating cycle. In addition, the modularity of the Kraken framework is highlighted by modeling the depletion of a 3D single fuel assembly with both Ants and Serpent based code systems. This capability can be used to assess the accuracy of nodal neutronics vs continuous energy Monte Carlo in the estimation of thermal margins. Finally, some possible topics for future work are introduced.

1. Introduction

VTT is in the process of replacing its old reactor analysis tools with a new set, Kraken (Leppänen et al., 2022). The Kraken framework consists of modular solvers for neutronics, thermal hydraulics and fuel behavior that are coupled through a central multi-physics driver Cerberus to provide reactor core simulator capabilities (Valtavirta and Tuominen, 2021). A further coupling can be made to system codes in order to model core–loop or core–plant transients (Tuominen et al., 2022). In order to build further expertise in core analysis, the framework builds largely on in-house solvers developed at VTT, although couplings to external solvers are also supported. While one large application for Kraken are the independent deterministic safety analyses of the Finnish nuclear power plants, the framework is also designed to be a flexible research tool that can be used for the design and evaluation of new reactor concepts (Leppänen et al., 2021).

The current methodology at VTT to evaluate thermal margins for PWRs is based on the analysis of isolated hot channels. In this multistep process time-dependent boundary conditions for the hot channels are obtained from a full core coupled transient calculation with 3D nodal neutronics and thermal hydraulics. The hot channel calculations are run with 1D thermal hydraulics without neutronics. For each hot channel the calculation is repeated while varying several parameters in order to provide conservative estimates for the thermal margins.

In this work, the goal is to start the development of an alternative best estimate type methodology for evaluating the thermal margins in a single coupled calculation by coupling nodal neutronics including pin power reconstruction to subchannel level thermal hydraulics and pin-by-pin fuel behavior. The following three codes are used: nodal neutronics code Ants, subchannel code SUBCHANFLOW and fuel behavior code SuperFINIX. The coupling of the three solvers is implemented with Python based multi-physics driver Cerberus. The first verification step in the development of the new methodology is the simulation of an operating cycle which is presented in this paper. The focus of this work is in the modeling of PWRs.

The capabilities of the developed coupled code system are demonstrated by modeling the first operating cycle of the Benchmark for Evaluation and Validation of Reactor Simulations (BEAVRS). The benchmark has been previously solved with numerous different code systems such as the Monte Carlo based MCS/CTF code system (Yu et al., 2020a,b) and the Virtual Environment for Reactor Applications (VERA) (Collins et al., 2020) which uses the transport solver MPACT. A brief comparison of calculated and measured critical boron concentrations is presented for the first cycle. Regarding the capability to evaluate thermal margins, maximum fuel centerline temperatures and minimum Departure from Nucleate Boiling Ratios (DNBR) are illustrated at three time points during the operating cycle.

By using the inherent modularity of the Kraken framework, the same coupled problem can be solved easily with both the Monte Carlo code Serpent and Ants in order to assess the accuracy of nodal neutronics vs continuous energy Monte Carlo in the estimation of thermal margins. This capability is demonstrated in this paper by modeling the

* Corresponding author.
E-mail address: riku.tuominen@vtt.fi (R. Tuominen).

https://doi.org/10.1016/j.anucene.2022.109447
Received 1 July 2022; Received in revised form 31 August 2022; Accepted 6 September 2022
Available online 18 September 2022

depletion of a 3D single fuel assembly with both Ants and Serpent based code systems.

2. Methods

2.1. Solvers

2.1.1. Serpent

Serpent (Leppänen et al., 2015b) is a Monte Carlo transport code developed at VTT Technical Research Centre of Finland since 2004. The code was originally written for spatial homogenization in reactor applications but has gained many additional features over the years of development. These include a built-in burnup calculation capability (Pusa and Leppänen, 2010), photon transport (Kaltiaisenaho, 2016) and a multi-physics interface which allows coupling to external CFD, thermal hydraulics and fuel performance codes (Leppänen et al., 2015a). A development version based on Serpent 2.2.0 was used in this work.

2.1.2. Ants

Ants (Sahlberg and Rintala, 2018; Rintala and Sahlberg, 2019a) is a nodal neutronics solver developed at VTT since 2017. The diffusion solution method in Ants is based on the analytic function expansion nodal method (AFEN) and flux expansion nodal method (FENM) (Noh and Cho, 1994; Xia and Xie, 2006). Rectangular, hexagonal and triangular geometries are supported. Ants is able to solve steady state, transient and burnup problems including microdepletion. Pin power reconstruction methodology is also supported (Rintala and Sahlberg, 2019b). Ants is currently used only at VTT and does not have a well established version numbering. The latest development version of Ants was used in the calculations.

2.1.3. SUBCHANFLOW

SUBCHANFLOW (SCF) is a subchannel thermal-hydraulic code developed at KIT (Imke and Sanchez, 2012). Both steady state and transient problems can be analyzed. The code solves liquid–vapor mixture equations for the conservation of mass, momentum and energy. In addition, the code can provide a solution for the heat conduction in the fuel rods and simplified models for cracking, swelling, gap conductance etc. are included. A modified SCF version based on SCF 3.6.1 was used in the calculations.

2.1.4. FINIX and SuperFINIX

FINIX (Ikonen et al., 2015) is a fuel behavior code developed at VTT since 2012. It solves the behavior of a single fuel rod in base irradiation and transient scenarios and has models for thermal–mechanical behavior of the fuel rod under transient conditions and extended irradiation periods. In order to obtain a core level solution, the behavior of multiple fuel rods (tens of thousands in full core pin-by-pin problems) has to be solved simultaneously and therefore, a wrapper code, SuperFINIX (Valtavirta et al., 2019) was developed. The wrapper runs a large number of individual FINIX solvers representing each unique fuel rod in the problem geometry. SuperFINIX supports parallelization using both OpenMP and MPI. SuperFINIX is currently used only at VTT and does not have a well established version numbering. In this work the latest development version of SuperFINIX was used.

2.2. Multi-physics driver Cerberus

Coupling of different solvers in VTT's reactor analysis framework Kraken is handled with Cerberus which is a Python based multi-physics driver. Cerberus communicates with solvers using sockets and enables access to solvers within the Python code. Functionalities needed in coupled calculations such as field transfer between codes, time stepping control and convergence checking are provided. Interpolation of field data between geometries of different codes is implemented using pre-generated interpolation matrices.

The solution flow in a Cerberus simulation is based on a model in which Cerberus sends predefined signals to solvers and upon receiving these signals the solvers complete tasks specified by the signals. The task can be exchanging field data with Cerberus, providing a new steady state solution for the current time point or moving to the next time point to give a few examples. Since Cerberus controls the solution flow and the solver must be able to communicate with Cerberus using sockets, source code modification is usually required in order to enable Cerberus simulations with a new solver.

2.3. Implementation of the coupling

The capability for coupled Cerberus calculations had been added to Serpent, Ants and SuperFINIX already before the work presented in this paper and therefore, most of the required new implementation was related to enabling Cerberus calculations with SCF and figuring out how to interpolate field data between the calculation geometries of the different codes. Fortunately, it was possible to utilize some of the work done already in the EU Horizon 2020 project McSAFE in which coupled full core burnup and transient problems were simulated with Monte Carlo neutronics, subchannel thermal-hydraulics and pin-by-pin fuel behavior solution (García et al., 2021a,c; Ferraro et al., 2020).

First of all, in the McSAFE project SCF was supplemented with a C API. By compiling SCF as a shared library and using this interface, the functionality of the code can be easily accessed from a program written in C/C++. Secondly, during the project a Python preprocessor was written for SCF. In addition to producing channel and rod connectivity data for SCF inputs, the preprocessor was also used for generating interpolation matrices required for interpolating field data between the calculation geometries of the codes that were coupled in the project. This functionality utilizes the MED module of the SALOME platform (CEA, 2022). Interpolation matrices between the different geometries of the coupled codes are acquired by creating a MED mesh for each of the geometries and utilizing the interpolation routines available in the MED library.

In practice, the Cerberus coupling of SCF was implemented by writing a simple wrapper code SCFWrap in C. The wrapper takes care of the socket communication with Cerberus. When a signal is received from Cerberus, the C interface of SCF is used to make calls to the SCF subroutines which are required to complete the task specified by the signal. The subroutines can be used for providing updated field data for the wrapper, calculating a new steady state solution etc. As long as the C interface does not change, an updated SCF version can be utilized without modifying the wrapper.

In order to generate interpolation matrices required in this work, the functionality of the SCF preprocessor was extended slightly. Since the interpolation relies on MED meshes, one or more meshes must be generated for each of the coupled codes. In Serpent calculations the temperature and density distributions of the coolant are defined on a subchannel level and fuel temperature distribution on a pin level. Two meshes are used, channel centered for the coolant and pin centered for the fuel. Power is tallied in the fuel mesh. Analogously to Serpent, separate meshes are needed for SCF for coolant and fuel. SuperFINIX requires only one mesh to describe the pin-wise distributions. For Ants two meshes are used. The first one is for the pin-wise power distribution calculated with pin power reconstruction. The second mesh corresponds to the nodalization of the diffusion solution and it is used for temperature and density distributions. At the moment, Ants uses a singular axial nodalization, which is used to represent and evaluate group constants, burnup distributions and serve as the domain for the flux solution. Mesh generation for Serpent and SCF was already available in the preprocessor but the capability to create meshes for SuperFINIX and Ants geometries was added.

The ready-made interpolation routines of the MED library were used to generate interpolation matrices based on the meshes for the different codes. In the interpolation of the density and temperature fields from a source mesh to a destination mesh, the value in the destination cell is calculated as a volume average of the values in the source cells which intersect the destination cell. In the interpolation of the power field, uniform power density is assumed in each source cell so that the power in the destination cell is simply calculated as a weighted sum of the powers in the source cells which intersect the destination cell. The weights are calculated by dividing the volumes of the intersections with the total volumes of the source cells. To be able to use the interpolation matrices in Cerberus calculations, an option to output the matrices in a Cerberus compatible file format was implemented to the SCF preprocessor.

In an effort to briefly verify that the Cerberus coupling of SCF works, a VVER assembly in steady state was modeled with SCF and Serpent. In addition to the Cerberus based solution, the test case was also solved using Interface for Code Coupling (ICoCo) based coupled Serpent-SCF system developed in the McSAFE project. The modeled VVER assembly was one of the test cases used in the project (García et al., 2020). Agreement between the results of the two coupled calculations was excellent. The obtained effective multiplication factors were agreeing within 2 pcm. The maximum absolute difference in fuel temperatures was approximately 2.4 K and in coolant temperatures 0.02 K.

2.4. Coupling scheme

The simulations presented in this work used constant extrapolation as a burnup algorithm for simplicity. This simple burnup algorithm assumes that the flux and cross sections remain at their beginning of step values throughout the burnup step. Both Serpent and Ants support also more advanced burnup algorithms. During the burnup calculation, at each time point a coupled steady state problem was solved with Picard iteration. On each coupled iteration the solution flow was the following. First, Ants or Serpent provided a new solution for neutronics and updated power field was transferred to SCF and SuperFINIX. Next, SCF provided a new solution for the coolant flow. The coolant temperature and density fields were transferred to Ants or Serpent. In addition, heat transfer coefficient and coolant temperature fields were transferred to SuperFINIX. Then, SuperFINIX provided a new solution for fuel rods and the fuel temperature field was transferred to Ants or Serpent. The fuel temperature field was based on effective fuel temperatures T_{eff} (Kozlowski and Downar, 2007) calculated on each axial level of each rod as:

$$T_{\text{eff}} = 0.7 \times T_{\text{surf}} + 0.3 \times T_{\text{center}},$$

where T_{center} is the centerline fuel temperature and T_{surf} the surface fuel temperature. Finally, convergence of the coupled problem was determined by comparing differences between the results (critical boron concentration, fuel temperature field and coolant temperature field) of two consecutive iterations against predefined criteria. In simulations with Ants also the internal convergence of the Ants solution (critical boron concentration iteration, fission source) was checked. The iteration of the coupled problem was stopped if convergence or predefined maximum number of iterations was reached.

It is worth emphasizing that Serpent used pin level fuel temperatures and channel level coolant temperatures and densities but in Ants the feedback was on nodal level. Here, the term channel level indicates that radially temperatures and densities were given separately for each subchannel between the fuel rods. Nodal level refers to the nodalization of the Ants solution and since 2 × 2 subnodalization was used, the fields were given radially on a quarter assembly level. As described in Section 2.3 the nodal level temperature and density fields were produced with volume averaging from the corresponding pin/channel level fields.

3. Test calculations

3.1. Group constant generation

Two group constants for Ants were generated with Serpent in the following manner:

- Fuel assemblies were homogenized in infinite lattice quarter assembly models with Fundamental Mode leakage correction applied based on a 70 group intermediate structure.
- Radial reflector was homogenized from a Serpent 2D full core model using superimposed universes to homogenize the radial reflector and the outermost sides of fuel assemblies into quarter assembly sized regions.
- The axial reflector was homogenized from a Serpent 3D full core simulation into cuboidal volumes on top and below of the 7 × 7 centermost assemblies in the core.

The fuel group constants were generated based on two sets of historical conditions corresponding to a nominal and off-nominal history. The group constants were evaluated at the nominal state point at 25 burnup points and the variation in group constants due to momentary variations in the thermal hydraulic conditions and coolant boron content was evaluated with 11 branch calculations off of the nominal point at 11 burnup points. The same branches were evaluated using both the nominal and off-nominal histories. Two energy groups were used.

The fuel assemblies used Cumulative Migration Method (CMM) (Liu et al., 2018) based diffusion coefficients. As there is no CMM formulation for homogenization problems where neutron tracks are not completely enclosed in the homogenized region, the diffusion coefficients in the reflector regions were based on the out scatter approximation with transport correction applied to ^{1}H in water.

The discontinuity factors of the fuel assembly quarters could be directly based on the Serpent solution as reflective boundary conditions were applied in the homogenization: The heterogeneous surface fluxes were tallied by Serpent and the homogeneous surface fluxes were based on the assembly mean heterogeneous flux as reflective boundary conditions mean that the homogeneous flux solution in such a system is spatially constant.

For the radial reflector nodes, the discontinuity factors were evaluated as described in Valtavirta et al. (2021): The heterogeneous surface fluxes were tallied directly from the Serpent solution and the homogeneous surface fluxes were obtained from a separate single node Ants calculation with group constant data and boundary conditions from the Serpent full core reflector homogenization calculation. The reflector side discontinuity factor was corrected by the ratio of the fuel side full core evaluated discontinuity factor and the fuel side infinite lattice assembly discontinuity factor as suggested in Smith (2017).

The evaluation of pin power form functions was conducted in the manner described in Valtavirta et al. (2021): The pin power form functions are evaluated as pin-cell heterogeneous power (due to flux in group g) per pin-cell homogeneous flux in group g multiplied by the system homogeneous macroscopic fission energy production cross section, i.e.

$$\text{FF}_{g,\text{pc}} = \frac{P^{\text{het}}_{g,\text{pc}}}{P^{\text{hom}}_{g,\text{pc}}} \tag{1}$$

where the subscript g refers to energy group and the subscript pc indicates that the power is calculated for the pin-cell. This is evaluated as

$$\text{FF}_{g,\text{pc}} = \frac{\int_{E_g^{\text{low}}}^{E_g^{\text{high}}} \int_{V_{\text{pc}}} \phi^{\text{het}}(\vec{r},E)\kappa(\vec{r},E)\Sigma_f(\vec{r},E)\mathrm{d}V\,\mathrm{d}E}{\int_{V_{\text{pc}}} \phi_g^{\text{hom}}\mathrm{d}V(\kappa\Sigma_f)_g}, \tag{2}$$

where the homogeneous flux solution used in the denominator is conducted with Ants and uses the same boundary conditions as the

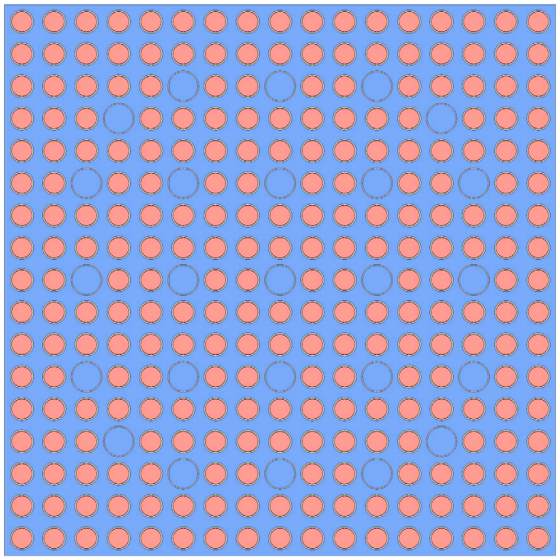

Fig. 1. XY geometry of the 3D single assembly case.

heterogeneous Serpent solution in the numerator. The homogenized fission energy production cross section here is the same as the one included in the group constant library.

The form functions can then be utilized in the nodal calculation to provide an estimate for the pin-cell heterogeneous power ($\hat{P}^{\text{het}}_{g,\text{pc}}$) based on the integrated homogeneous power for the pin-cell:

$$\hat{P}^{\text{het}}_{g,\text{pc}} = \text{FF}_{g,\text{pc}} P^{\text{hom}}_{g,\text{pc}} = \text{FF}_{g,\text{pc}} \int_{V_{\text{pc}}} \phi^{\text{hom}}_g \text{d}V (\kappa\Sigma_f)_g. \tag{3}$$

3.2. 3D single assembly Serpent vs Ants

3.2.1. Description

The geometry for the test case was modified from the fuel assembly geometry used in the BEAVRS benchmark. Fuel composition in the modeled assembly corresponds to the 1.6 % enriched fuel of the benchmark. Control rods are not included and there are no burnable absorber rods. Structures below and above active fuel were taken unmodified from the BEAVRS benchmark. Active fuel length was reduced from 365.76 cm to 200 cm to make the system smaller in order to reduce statistical uncertainty in the Serpent calculation. Three spacer grids were placed within the active fuel region. Serpent geometry is presented in Figs. 1 and 2. Reflective boundary condition was used radially and vacuum boundary condition axially. Total power was set to 9.66 MW, inlet temperature to 566.48 K, inlet flow rate to 45.98 kg/s and outlet pressure to 15.5132 MPa. Inlet temperature and outlet pressure have been taken directly from BEAVRS. Total power was calculated based on the average linear power of the BEAVRS core. The ratio of total power and inlet flow rate is equal to the corresponding value evaluated for BEAVRS.

Axially the active region was divided into 21 nodes in the Ants model. In addition, there were 4 bottom and 7 top reflector nodes. Radially the assembly was divided with 2 × 2 subnodalization. In the Serpent model the fuel was divided into 20 burnup zones in the axial direction. The division corresponded to the one used in Ants apart from the bottommost burnup zone which combined the two bottommost nodes. The height of the bottommost node in Ants was very small and using the same burnup zone height in Serpent would have resulted in very poor statistics. Radially pin-by-pin burnup zone division was used in Serpent and each pin was further divided into two radial zones with a 0.3 mm surface layer and the center as separate zones. In order to reduce the number of depletion zones, 1/8 symmetry of the assembly

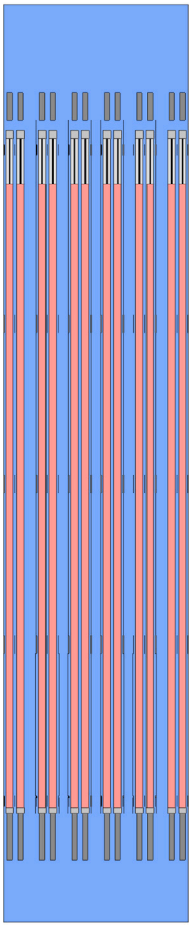

Fig. 2. XZ geometry of the 3D single assembly case.

was accounted for in the Serpent model with universe symmetry option. SCF model had coolant-centered subchannels and SuperFINIX solved each fuel rod separately. SCF and SuperFINIX models used 36 axial layers.

With both code systems the assembly was depleted at full power up to 220 effective full power days (EFPD) corresponding to an average burnup of 9.2 MW d/kg U. The following depletion history given in EFPD was used: 0, 1, 5, 10, 20, 30, 40, 60, 80, 100, 120, 140, 160, 180, 200, 220. Both Serpent and Ants were set to iterate critical boron concentration. The following convergence criteria were used for checking the convergence of the coupled solution at each time point: 1 ppm for critical boron concentration, 1 K for local fuel temperature and 1 kg/m^3 for local coolant density. Maximum number of coupled iterations was set to 10.

In order to estimate the statistical uncertainty in the Serpent based solution, the test case was simulated 4 times with different random number seeds. Serpent simulated 250 million active neutron histories in each transport calculation and a stochastic approximation based relaxation scheme (Dufek and Gudowski, 2006) was used for the tallied power distribution.

3.2.2. Results

The Serpent based simulations were run on computer nodes with 128 cores and the total calculation time for each repetition was approximately one week. The Ants based simulation finished in a couple of minutes on a laptop. By looking at the convergence of the Serpent simulations, it can be stated that the convergence criteria of 1 ppm was slightly too tight considering the magnitude of the statistical

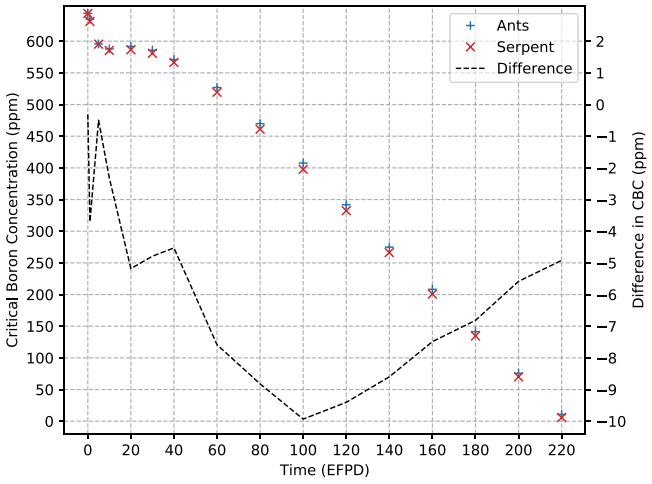

Fig. 3. Predicted critical boron concentrations in the Ants and Serpent based simulations along with the difference in the predicted CBCs.

uncertainty. Under-relaxation was not applied to the critical boron concentration between coupled iterations and therefore its convergence was limited by the statistical uncertainty of a single transport calculation. In a couple of time points the convergence criteria for the fuel and coolant fields were clearly met but due to statistical fluctuation the difference in critical boron was higher than 1 ppm which resulted in additional coupled iterations.

Comparison of critical boron concentrations (CBCs) during the simulated cycle is presented in Fig. 3. For Serpent mean values calculated based on the 4 repetitions are used. Estimated standard errors of the mean were below 0.5 ppm for all time points. Ants overpredicts CBC compared to Serpent at each time point. At the beginning of the cycle (BOC) the CBCs are very close to each other and they differ by approximately 0.3 ppm. Larger differences are observed later on during the cycle and the maximum absolute difference is approximately 9.9 ppm at 100 EFPD. After this point the absolute difference decreases until EOC.

Table 1 presents differences in power, (effective) fuel temperature and coolant temperature fields between Ants and Serpent based simulations at BOC and EOC. Maximum (MAX) and root mean square (RMS) differences are listed for each field. The differences were calculated independently between the results of the Ants based simulation and the results of each Serpent repetition, and the minimum and maximum differences taken over the repetitions are shown. For the power field these differences are relative differences. For the fuel and coolant temperature fields absolute differences are shown. Pin/channel level fields are used in the comparisons. In addition, maximum centerline temperatures and minimum DNBRs are shown. It is worth noting that they are taken over the whole assembly separately for Serpent repetitions and Ants, and the maximum/minimum values are not necessarily in the same pin in the Ants and Serpent based simulations.

First of all, differences in minimum DNBRs are negligible at BOC and less than 0.1 at EOC. For the maximum fuel centerline temperature differences are less than 2 K at BOC and at EOC the maximum difference between the Serpent repetitions and Ants is approximately 16 K. Differences in the coolant temperatures are negligible but larger differences are observed for the power and fuel temperature fields.

Some differences are expected since the thermal feedback and the accumulation of burnup are handled differently in Serpent and Ants. In Serpent the thermal feedback is modeled explicitly using the pin/channel level fields. In Ants, however, the thermal feedback is on quarter assembly level and originates from the parametrization of the group constants. It cannot capture the effect of varying thermal hydraulics conditions on a pin/channel level. Regarding the modeling of fuel burnup, Serpent accumulates burnup separately for each fuel pin but in Ants burnup is accumulated on a quarter assembly level. It is also worth noting, that some of the observed differences in the results may be due to the statistical uncertainty in the Serpent based calculations since the number of simulated neutron histories was somewhat limited due to high computational requirements of the coupled burnup calculation. For all presented quantities in Table 1 the differences between Ants and Serpent are larger at EOC compared to BOC. The differences originating from different handling of thermal feedback and burnup accumulate during the cycle.

Even though some differences were observed between the results of the two code systems, it can be stated that the agreement in general was good for this simple test case. In the future, a more realistic comparison can be made for example by simulating an SMR core. The limiting factor in these comparisons is naturally the high computational requirement of the Monte Carlo transport especially since pin power estimates with low statistical uncertainties are required.

3.3. Simulation of the first operating cycle of BEAVRS

3.3.1. Description

BEAVRS (M.I.T. Computational Reactor Physics Group, 2020) is a PWR full core benchmark based on a commercial nuclear reactor. It provides a detailed description of the reactor geometry and measured data for the initial two cycles of the reactor. Since the full benchmark documentation is available online, the specifications are not covered here in detail. In this work revision 2.0.2 from 10/30/17 was used.

The BEAVRS core consists of 193 square 17 × 17 fuel assemblies. During the first cycle the fuel enrichment in each of the assemblies is 1.6, 2.4 or 3.1%. Part of the assemblies contain borosilicate burnable absorber rods. The central guide tube for 58 assemblies is filled by an instrument tube instead of water. Since these assemblies are not located symmetrically the core is slightly asymmetrical. However, in this work the instrument tubes were not included and a symmetrical core was used instead.

Radially the Ants model consisted of the active core and one assembly-wide of radial reflector. Axially the entire extent of the benchmark model was covered. Ants does not currently support axial rehomogenization and therefore the model used an axial discretization originating from the axial zone division presented in the benchmark documentation. In total there were 51 axial nodes: 4 of which were located in the bottom reflector, 40 in the active core and 7 in the top reflector. Radially 2 × 2 subnodalization was used in each assembly. The Ants model included also control rods but they were fully extracted in the simulation. Equilibrium Xenon was used.

The SCF model of the core used coolant-centered subchannels and in total there were 56288 channels. SuperFINIX solved each of the 50952 fuel rods separately. Both SCF and SuperFINIX used identical axial discretization with 63 layers. The discretization was modified from the axial discretization of the active core in the Ants model by splitting and combining axial nodes in order to make the layer heights more uniform.

The detailed power history provided in the benchmark documentation was used in the simulation of the first operating cycle. Fig. 4 shows the power history which consisted of 344 time points. The nominal power of the reactor was 3411 MW. The following criteria were used for checking the convergence of the coupled solution at each time point: 0.5 ppm for critical boron concentration, 0.1 K in L^2-norm for fuel temperature and 0.1 kg/m^3 in L^2-norm for coolant density. Maximum number of coupled iterations was set to 10 and during the iteration under-relaxation was applied to the power field with a factor of 0.7.

3.3.2. Coupled calculation performance

The simulation was run on a computer node consisting of two Twenty-Core Intel Xeon Gold 6248 2.5 GHz processors with 384 GB RAM memory. All of the codes used OpenMP parallelization with 40 threads. It is worth noting that parallel scalability of SCF is quite poor and based on very brief testing the calculation time required by SCF was

Table 1
Differences in selected quantities between Ants and Serpent based simulations at BOC and EOC.

	Power		Fuel temperature		Coolant temperature		Max centerline (K)		Min DNBR	
	MAX (%)	RMS (%)	MAX (K)	RMS (K)	MAX (K)	RMS (K)	Serpent	Ants	Serpent	Ants
BOC	3.28/3.98	0.60/0.69	3.55/3.79	1.00/1.23	0.07/0.08	0.03/0.04	1459.2/1460.3	1458.7	3.04/3.05	3.05
EOC	4.18/4.64	1.37/1.62	16.16/17.37	3.67/4.85	0.24/0.29	0.13/0.16	1203.2/1211.4	1218.8	3.60/3.61	3.67

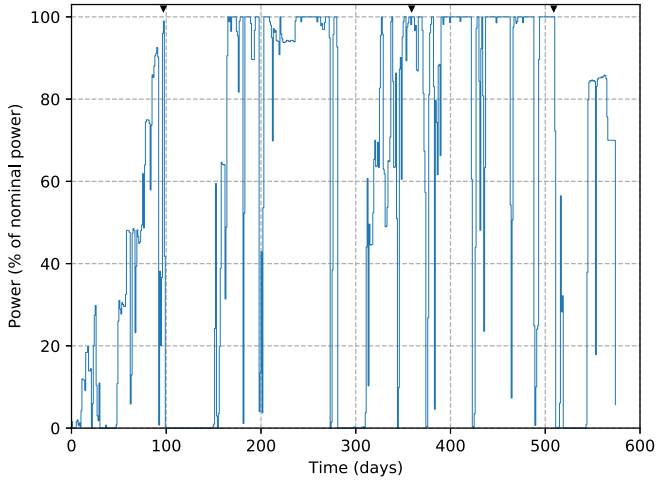

Fig. 4. Power history for the simulation. The black triangles placed at 97, 359 and 509 days indicate the time points for which pin/channel-level results are shown in Section 3.3.4.

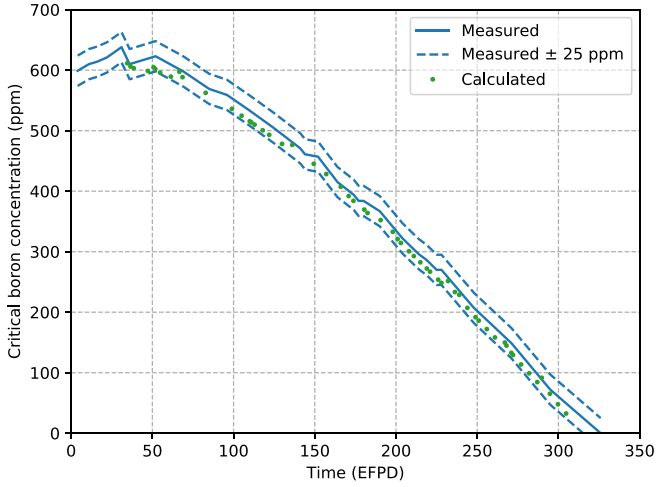

Fig. 5. Calculated critical boron concentrations and measured critical boron concentrations with 25 ppm margins for the first operating cycle of BEAVRS.

only approximately halved when the number of threads was increased from 1 to 40. Total calculation time for the coupled simulation was ~ 78 h. The calculation times of different solvers were of the same order and Ants used the least amount of time.

In 331 of the total of 344 time points convergence was reached in 5 or less coupled iterations. However, problems were encountered when iterating coupled steady state solution for some of the time points. In 3 time points at 463, 465 and 516 days with total powers of 1851 MW, 1727 MW and 1927 MW, respectively, convergence was not reached within the maximum 10 coupled iterations. More specifically, the convergence criterion for the fuel temperature was not met. On the last coupled iteration the L^2-norms for the fuel temperature were 0.103 K, 0.102 K and 0.195 K in the three time points with convergence issues. In addition, in some of the time points in which the coupled solution converged, maximum local difference in the fuel temperature between the last and second-to-last coupled iteration was still a couple of Kelvins. It was also observed that the average calculation time required by SuperFINIX to produce a new steady state solution varied heavily between different time points. The minimum average time was ~ 5 s and maximum ~ 1000 s. Even though the convergence issue only has a minor effect on the temperature distributions of some individual rods at a few time points, the cause of the problem should be investigated in the future.

3.3.3. Critical boron

Fig. 5 shows the calculated and measured critical boron concentrations during the first operating cycle. For the measurements 25 ppm margins have been also drawn in order to illustrate the magnitude of differences between calculated and measured CBCs. Calculated CBCs are presented only for time points when the reactor is at full power. CBC is underpredicted throughout the cycle apart from one point at ~ 290 EFPD and the differences stay within the 25 ppm margins. CBC is also underpredicted in the simulations presented in Yu et al. (2020a) and Collins et al. (2020) but the underprediction is smaller in the Ants based simulation. For Yu et al. (2020a) the differences between measured and calculated CBCs are not explicitly given but by looking at Fig. 4 of the article the underprediction is clearly larger at least for the first half of the cycle with differences of approximately 50 ppm for several time points. In Collins et al. (2020) the underprediction is mostly between approximately 25 ppm and 45 ppm.

3.3.4. Selected pin/channel-level results

The simulation produced various data on pin/channel-level for the operating cycle. As an example minimum DNBRs and maximum fuel centerline temperatures are illustrated in Figs. 6–9. The data is presented for three time points at 97, 359 and 509 days after BOC corresponding to 27.4, 173.8 and 304.7 EFPD, respectively. At 359 and 509 days the reactor was at the nominal power of 3411 MW. At 97 days the total power was slightly smaller and approximately 3376 MW. The three time points are indicated with black triangles in Fig. 4 which shows the power history. The DNBRs and fuel temperatures shown here are intended only for demonstrating the pin/channel-level data that can be obtained from these kind of simulations. Their values depend on several modeling options such as the choice of critical heat flux correlation etc. which may not be optimal in the simulation presented here.

Maximum fuel centerline temperature distributions are presented in Figs. 6–8. One quarter of the core is shown. However, it is worth noting that due to symmetry it would be sufficient to show only one eighth of the core. For each rod the maximum fuel centerline temperature along the entire length of the rod is presented. The labels indicating the positions of the assemblies correspond to the ones used in the benchmark documentation.

At 97 days the maximum fuel centerline temperature is 1677 K. In Fig. 6 two rods share this maximum temperature due to 1/8 symmetry of the core. The rods are located near the center of the assembly in position D12. Fuel enrichment in this assembly is 2.4% and it does not contain burnable absorber rods.

During the cycle the radial power distribution becomes more uniform due to depletion of burnable absorbers and faster accumulation of burnup in the assemblies with higher initial power. The maximum fuel centerline temperature decreases to 1434 K at 359 days. Two rods

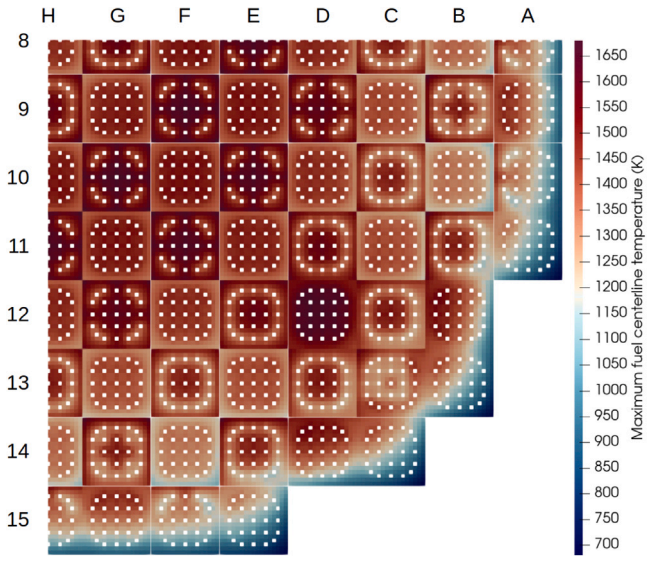

Fig. 6. Maximum fuel centerline temperature distribution at 97 days.

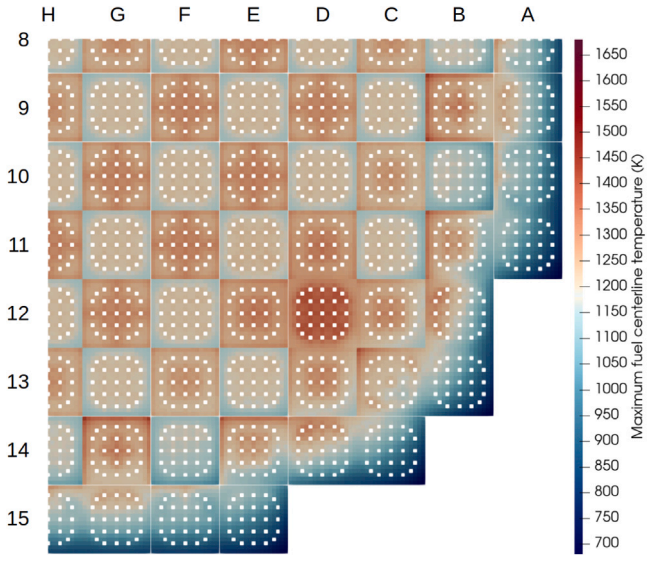

Fig. 7. Maximum fuel centerline temperature distribution at 359 days.

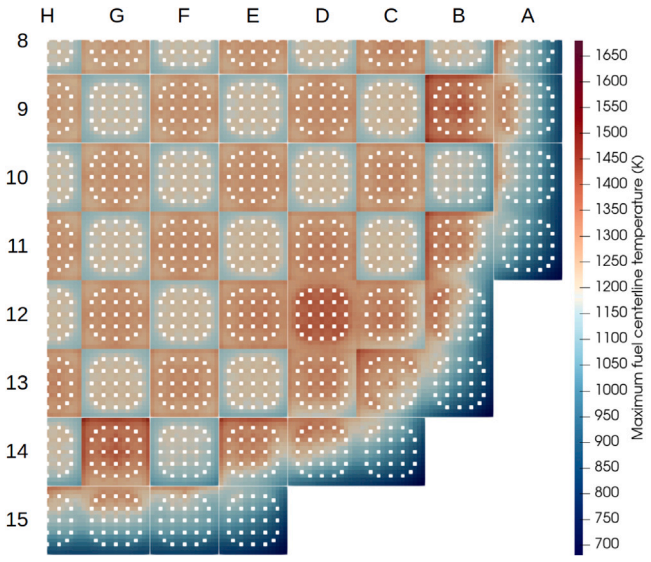

Fig. 8. Maximum fuel centerline temperature distribution at 509 days.

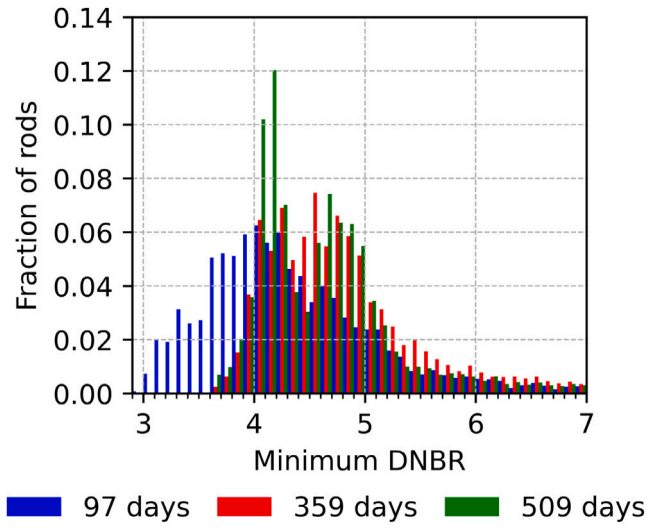

Fig. 9. Histogram of minimum rod-wise DNBRs at 97, 359 and 509 days.

which share this maximum temperature are in assemblies at positions B9 and G14 in Fig. 7. In both assemblies the rod is located at the top-left corner of the assembly. Fuel enrichment in these assemblies is 3.1% and they contain 20 burnable absorber rods.

Finally, at 509 days the maximum fuel centerline temperature is 1469 K and slightly higher than at 359 days. The maximum temperature is reached in the same rods as at 359 days.

A histogram of minimum rod-wise DNBRs at the three selected time points is presented in Fig. 9. In order to create the histogram minimum DNBR along the entire length of the rod was calculated for each fuel rod at each time point. In the histogram the upper limit for the last bin was set to 7. At each time point the rod-wise minimum DNBR is lower than this upper limit for approximately 90 percent of the rods.

Similarly as in the maximum fuel temperature distributions, the flattening of the power distribution during the operating cycle can also be observed in the DNBR histogram with lower rod-wise minimum DNBR values near the beginning of cycle at 97 days when the power distribution is more peaked. The minimum DNBRs for 97, 359 and 509 days are 2.96, 3.56 and 3.42, respectively.

4. Conclusions and future work

In this work the nodal neutronics code Ants was coupled with subchannel code SUBCHANFLOW and fuel behavior solver SuperFINIX in the Kraken framework. The coupled code system was used to model the first operating cycle of the BEAVRS benchmark and selected results were presented. In addition, the modularity of the Kraken framework was demonstrated by modeling the depletion of a single fuel assembly with both Ants and Serpent based code systems.

There are multiple topics for future work. First of all, the convergence issues with SuperFINIX should be studied further. Secondly, up to now the presented coupled code system has only been used to model depletion. However, typically in safety analyses the thermal margins should be evaluated during transient scenarios. The capability to model transients is mostly already available but some additional work is required related to exchanging boundary conditions between fuel behavior and thermal hydraulics in time dependent calculations. In the near future the code system will be used to model a rod ejection transient in NuScale core in EU Horizon 2020 project McSAFER (Sanchez-Espinoza et al., 2021).

Thirdly, a more realistic test case than the single assembly presented in this paper could be simulated with both Serpent and Ants based code systems to estimate the magnitude of expected error in pin-level safety parameters originating from the use of nodal neutronics. Since the computational requirement for coupled depletion with Serpent is high, a SMR core could be a suitable test case.

Finally, some kind of a coarsening method such as the one presented in García et al. (2021b) could be applied to the calculation geometry to speed up the simulations. The basic idea in the coarsening is to model the most interesting regions of the geometry such as the assembly with the highest power on a pin/subchannel level and other regions with lower fidelity with one representative fuel rod/channel for each assembly or quarter assembly.

CRediT authorship contribution statement

Riku Tuominen: Conceptualization, Methodology, Software, Formal analysis, Investigation, Writing – original draft, Writing – review & editing, Visualization. **Ville Valtavirta:** Conceptualization, Software, Writing – original draft, Writing – review & editing.

Declaration of competing interest

The authors declare that they have no known competing financial interests or personal relationships that could have appeared to influence the work reported in this paper.

Data availability

Data will be made available on request.

Acknowledgments

The authors would like to acknowledge the help of U. Imke with the SCF source code modifications and the previous work of M. García related to SCF preprocessor and SCF C API. This work has received funding from the LONKERO project, Finland under the Finnish National Research Programme on Nuclear Power Plant Safety, SAFIR2022.

References

CEA, 2022. MEDCoupling 7.8.0 documentation. URL: https://docs.salome-platform.org/7/dev/MEDCoupling/index.html (Accessed 24 August 2022).

Collins, B., Godfrey, A., Stimpson, S., Palmtag, S., 2020. Simulation of the BEAVRS benchmark using VERA. Ann. Nucl. Energy 145, 107602. http://dx.doi.org/10.1016/j.anucene.2020.107602, URL: https://www.sciencedirect.com/science/article/pii/S0306454920303005.

Dufek, J., Gudowski, W., 2006. Stochastic approximation for Monte Carlo calculation of steady-state conditions in thermal reactors. Nucl. Sci. Eng. 152, 274–283.

Ferraro, D., García, M., Valtavirta, V., Imke, U., Tuominen, R., Leppänen, J., Sanchez-Espinoza, V., 2020. Serpent/SUBCHANFLOW pin-by-pin coupled transient calculations for the SPERT-IIIE hot full power tests. Ann. Nucl. Energy 142, 107387. http://dx.doi.org/10.1016/j.anucene.2020.107387, URL: https://www.sciencedirect.com/science/article/pii/S0306454920300852.

García, M., Bilodid, Y., Basualdo Perello, J., Tuominen, R., Gommlich, A., Leppänen, J., Valtavirta, V., Imke, U., Ferraro, D., Van Uffelen, P., Seidl, M., Sanchez-Espinoza, V., 2021a. Validation of Serpent-SUBCHANFLOW-TRANSURANUS pin-by-pin burnup calculations using experimental data from a Pre-Konvoi PWR reactor. Nucl. Eng. Des. 379, 111173. http://dx.doi.org/10.1016/j.nucengdes.2021.111173, URL: https://www.sciencedirect.com/science/article/pii/S0029549321001254.

García, M., Ferraro, D., Valtavirta, V., Tuominen, R., Imke, U., Mercatali, L., Sanchez-Espinoza, V., Leppänen, J., 2021b. A subchannel coarsening method for Serpent2-SUBCHANFLOW applied to a full-core VVER problem. EPJ Web Conf. 247, 06018. http://dx.doi.org/10.1051/epjconf/202124706018.

García, M., Tuominen, R., Gommlich, A., Ferraro, D., Valtavirta, V., Imke, U., Van Uffelen, P., Mercatali, L., Sanchez-Espinoza, V., Leppänen, J., Kliem, S., 2020. A Serpent2-SUBCHANFLOW-TRANSURANUS coupling for pin-by-pin depletion calculations in light water reactors. Ann. Nucl. Energy 139, 107213. http://dx.doi.org/10.1016/j.anucene.2019.107213, URL: https://www.sciencedirect.com/science/article/pii/S0306454919307236.

García, M., Voka, R., Tuominen, R., Gommlich, A., Leppänen, J., Valtavirta, V., Imke, U., Ferraro, D., Van Uffelen, P., Milisdörfer, L., Sanchez-Espinoza, V., 2021c. Validation of Serpent-SUBCHANFLOW-TRANSURANUS pin-by-pin burnup calculations using experimental data from the Temelín II VVER-1000 reactor. Nucl. Eng. Technol. 53, 3133–3150. http://dx.doi.org/10.1016/j.net.2021.04.023, URL: https://www.sciencedirect.com/science/article/pii/S1738573321002424.

Ikonen, T., Loukusa, H., Syrjälahti, E., Valtavirta, V., Leppänen, J., Tulkki, V., 2015. Module for thermomechanical modeling of LWR fuel in multiphysics simulations. Ann. Nucl. Energy 84, 111–121. http://dx.doi.org/10.1016/j.anucene.2014.11.004, URL: http://www.sciencedirect.com/science/article/pii/S0306454914005842.

Imke, U., Sanchez, V.H., 2012. Validation of the subchannel code SUBCHANFLOW using the NUPEC PWR tests (PSBT). Sci. Technol. Nucl. Install. 2012.

Kaltiaisenaho, T., 2016. Implementing a photon physics model in Serpent 2 (M.Sc. thesis). Aalto University.

Kozlowski, T., Downar, T.J., 2007. PWR MOX/UO_2 Core Transient Benchmark, Final Report. Technical Report NEA/NSC/DOC(2006)20.

Leppänen, J., Hovi, V., Ikonen, T., Kurki, J., Pusa, M., Valtavirta, V., Viitanen, T., 2015a. The numerical multi-physics project (NUMPS) at VTT technical research centre of Finland. Ann. Nucl. Energy 84, 55–62.

Leppänen, J., Pusa, M., Viitanen, T., Valtavirta, V., Kaltiaisenaho, T., 2015b. The Serpent Monte Carlo code: Status, development and applications in 2013. Ann. Nucl. Energy 82, 142–150.

Leppänen, J., Valtavirta, V., Rintala, A., Hovi, V., Tuominen, R., Peltonen, J., Hirvensalo, M., Dorval, E., Lauranto, U., Komu, R., 2022. Current status and on-going development of VTT's Kraken core physics computational framework. Energies 15, http://dx.doi.org/10.3390/en15030876, URL: https://www.mdpi.com/1996-1073/15/3/876.

Leppänen, J., Valtavirta, V., Tuominen, R., Rintala, A., Lauranto, U., 2021. A Finnish district heating reactor: Neutronics design and fuel cycle simulations. In: Proc. ICONE28. Virtual, Online.

Liu, Z., Smith, K., Forget, B., Ortensi, J., 2018. Cumulative migration method for computing rigorous diffusion coefficients and transport cross sections from Monte Carlo. Ann. Nucl. Energy 112, 507–516. http://dx.doi.org/10.1016/j.anucene.2017.10.039, URL: http://www.sciencedirect.com/science/article/pii/S0306454917303778.

M.I.T. Computational Reactor Physics Group, 2020. BEAVRS benchmark web page. URL: https://crpg.mit.edu/research/beavrs.

Noh, J.M., Cho, N.Z., 1994. A new approach of analytic basis function expansion to neutron diffusion nodal calculation. Nucl. Sci. Eng. 116, 165–180. http://dx.doi.org/10.13182/NSE94-A19811.

Pusa, M., Leppänen, J., 2010. Computing the matrix exponential in burnup calculations. Nucl. Sci. Eng. 164, 140–150. http://dx.doi.org/10.13182/NSE09-14.

Rintala, A., Sahlberg, V., 2019a. Extension of nodal diffusion solver of Ants to hexagonal geometry. Kerntechnik 84, 252–261.

Rintala, A., Sahlberg, V., 2019b. Pin power reconstruction method for rectangular geometry in nodal neutronics program Ants. In: Proceedings of the International Conference Nuclear Energy for New Europe, PortoroŽ, Slovenia, September 9–12, 2019. URL: http://www.nss.si/nene2019/.

Sahlberg, V., Rintala, A., 2018. Development and first results of a new rectangular nodal diffusion solver of Ants. In: Proc. PHYSOR 2018. Cancun, Mexico.

Sanchez-Espinoza, V.H., Gabriel, S., Suikkanen, H., Telkkä, J., Valtavirta, V., Bencik, M., Kliem, S., Queral, C., Farda, A., Abéguilé, F., Smith, P., Uffelen, P.V., Ammirabile, L., Seidl, M., Schneidesch, C., Grishchenko, D., Lestani, H., 2021. The H2020 McSAFER project: Main goals, technical work program, and status. Energies 14, http://dx.doi.org/10.3390/en14196348, URL: https://www.mdpi.com/1996-1073/14/19/6348.

Smith, K., 2017. Nodal diffusion methods and lattice physics data in LWR analyses: Understanding numerous subtle details. Prog. Nucl. Energy 101, 360–369. http://dx.doi.org/10.1016/j.pnucene.2017.06.013, URL: http://www.sciencedirect.com/science/article/pii/S0149197017301609.

Tuominen, R., Komu, R., Valtavirta, V., 2022. Coupling of TRACE with nodal neutronics code Ants using the exterior communications interface and VTT's multiphysics driver Cerberus (submitted). In: Proceedings of PHYSOR 2022. Pittsburgh, PA.

Valtavirta, V., Peltonen, J., Lauranto, U., Leppänen, J., 2019. SuperFINIX – A flexible-fidelity core level fuel behavior solver for multi-physics applications. In: NENE 2019. Portorož, Slovenia.

Valtavirta, V., Rintala, A., Lauranto, U., 2021. Validating the Serpent-Ants calculation chain using BEAVRS fresh core hot zero power data. J. Nucl. Eng. Rad. Sci. http://dx.doi.org/10.1115/1.4052731.

Valtavirta, V., Tuominen, R., 2021. A simple reactor core simulator based on VTT's Kraken computational framework. In: Proceedings of ANS M&C 2021. Raleigh, North Carolina, USA.

Xia, B., Xie, Z., 2006. Flux expansion nodal method for solving multigroup neutron diffusion equations in hexagonal-z geometry. Ann. Nucl. Energy 33, 370–376. http://dx.doi.org/10.1016/j.anucene.2005.06.011, URL: https://www.sciencedirect.com/science/article/pii/S0306454905002240.

Yu, J., Lee, H., Kim, H., Zhang, P., Lee, D., 2020a. Coupled neutronics–thermal-hydraulic simulation of BEAVRS cycle 1 depletion by the MCS/CTF code system. Nucl. Technol. 206, 728–742. http://dx.doi.org/10.1080/00295450.2019.1677107.

Yu, J., Lee, H., Kim, H., Zhang, P., Lee, D., 2020b. Simulations of BEAVRS benchmark cycle 2 depletion with MCS/CTF coupling system. Nucl. Eng. Technol. 52, 661–673. http://dx.doi.org/10.1016/j.net.2019.09.007, URL: https://www.sciencedirect.com/science/article/pii/S173857331930110X.